PROCEEDINGS OF SCIENCE

Superhumps and their Relation to the Disk Instability Model

Daisaku Nogami[a,*]

[a] *Department of Astronomy, Graduate Schoold of Science, Kyoto University,*
Kitashirakawa Oiwake-cho, Sakyo-ku, Kyoto 606-8502, Japan

E-mail: nogami@kusastro.kyoto-u.ac.jp

Since the discovery of superhumps in 1974, these photometric modulations have provided a crucial observational window into disk instabilities in cataclysmic variable stars, particularly the tidal instability associated with the 3:1 resonance. Over the past few decades, extensive time-resolved photometry has revealed a rich diversity of superhump-related phenomena, including delayed superhump development, early superhumps in WZ Sge-type dwarf novae, systematic stage A-B-C evolution, negative superhumps, and superhumps observed in related systems such as intermediate polars and AM CVn stars.

In this invited review, we summarize key observational advances since the establishment of the thermal-tidal instability framework, discuss their theoretical interpretations within the disk instability model, and highlight remaining open problems. These developments have been driven by coordinated networks of amateur observers, wide-field robotic surveys, and continuous high-precision space-based photometry from Kepler and TESS. Together, they demonstrate that superhumps remain a powerful probe of disk dynamics, binary parameters, and the interplay between thermal, tidal, and geometric effects in accretion disks.

87th Fujihara Seminar: The 50th Anniversary Workshop of the Disk Instability Model in Compact Binary Stars (DIM50TH2025)
22-26 September 2025
Tomakomai, Japan

PoS(DIM50th2025)010

---

[*] Speaker

© Copyright owned by the author(s) under the terms of the Creative Commons Attribution-NonCommercial-NoDerivatives 4.0 International License (CC BY-NC-ND 4.0) All rights for text and data mining, AI training, and similar technologies for commercial purposes, are reserved. ISSN 1824-8039 . Published by SISSA Medialab.

PoS(DIM50th2025)010

1. Introduction

Cataclysmic variable stars (CVs) consist of a late-type main sequence star (secondary star) and a white dwarf (primary star) surrounded by an accretion disk formed by gas transferred from the secondary star ([1] for a review). Dwarf novae (DNe) are a class of CVs that undergo outbursts caused by the thermal instability [2].

Superhumps were first discovered in a dwarf nova VW Hyi by Vogt [3] in 1974 and have been studied extensively by many researchers since then. Superhumps are observed only during superoutbursts and are characterized by their period typically a few percent longer than the orbital period and the small amplitude of typically 0.1–0.3 mag [4]. They are visible even in pole-on systems, crucially indicating that they are non-geometrical in origin. The memorable book by Warner [1] describes almost all of the phenomena observed in cataclysmic variable stars in the literature by 1995, including superoutbursts and superhumps in SU UMa stars.

The theoretical explanation for superhumps lies in the beat phenomenon between the orbital motion and the precession of an eccentric disk [5]. This eccentricity is caused by the tidal instability related to the 3:1 resonance in the accretion disk. This mechanism is central to the definition of SU UMa-type dwarf novae.

The review by Osaki [6] summarizes the thermal-tidal instability (TTI) model for dwarf nova outbursts which had been established by 1996 in a framework connecting normal outbursts due solely to the thermal instability and superoutbursts due to a conbination of thermal and tidal instabilities (see also [7]). The most important figure in this review is shown in Fig. 1. The behavior of these systems is largely governed by the mass transfer rate ($\dot{M}_{\rm tr}$) and the orbital period ($P_{\rm orb}$):

- **Nova-likes / Permanent superhumpers:** High $\dot{M}_{\rm tr}$ leads to stable disks. The latter is tidally unstable and always shows superhumps.

- **Z Cam / SS Cyg:** Intermediate/low $\dot{M}_{\rm tr}$ results in systems dominated by thermal instability. Z Cam stars are around the border line of the thermal instabiliy and sometimes show a standstill

- **ER UMa / SU UMa / WZ Sge:** Short $P_{\rm orb}$ (low mass ratio q) allows the disk to reach the 3:1 resonance, triggering tidal instability. Larger $\dot{M}_{\rm tr}$ systems, namely ER UMa > SU UMa > WZ Sge, have shorter superoutburst-recurrence cycle.

In section 2, we summarize recent observational results of superhumps in CVs, theoretical interpretation and remaining problems. A brief summary is put in section 3.

2. Observations and Theoretical Explanations of Superhumps and related phenomena

This section examines several observational results concerning superhumps in recent years that are difficult to explain by theories up to 1996, and present their current theoretical interpretations and remaining problems.

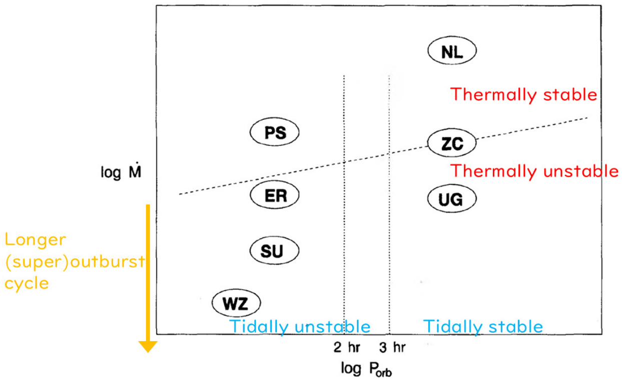

Figure 1: $\dot{M}$-P_{orb} diagram. The acronyms of NL, ZC, UG, PS, ER, SU and WZ present nova-likes, Z Cam-type stars, U Gem(SS Cyg)-type stars, permanent superhumpers, ER UMa-stars, SU UMa-stars and WZ Sge-type stars. CVs in the upper and lower regions separated by the oblique line are thermally stable and unstable, respectively. CVs in the right and left regions are tidally stable and unstable, respectively. Systems with lower mass transfer rates have longer (super)outburst-recurrence cycles. This figure was created based on Figure 3 in [6].

2.1 Superhump Evolution

While earlier studies (e.g., [8]) analyzed the superhump evolution, long-term coverage was often insufficient to systematically discuss that evolution. More recent systematic studies ([9], and its series of papers), however, have identified three distinct stages of superhump evolution:

1. **Stage A:** Characterized by a constant long period and growing amplitude.
2. **Stage B:** The superhump period becomes shorter initially, which then lengthens while the amplitude decays in most cases. This represents the propagation of the eccentricity wave to the inner part of the disk.
3. **Stage C:** Characterized by a constant short period. This stage typically appears around the end of the superoutburst and is accompanied by an decrease of the decline rate.

An example is shown in figure 2.

This course of superhump evolution is explained by the DIM [10]. The stage A is the growing period of the superhumps as the eccentric deformation remains at the 3:1 resonance radius. The period of the stage-A superhump thus represents the precession rate at the 3:1 resonance radius. During the stage B, the eccentricity wave probagetes to the inner part of the disk. The period of the stage-B superhump represents the overall precession rate of the disk. However, the remaining problem is how the lengthening of the stage-B superhump period is explained. Note that some systems show constancy or even shortening of the stage-B superhump period. Furthermore, there are problems regarding the stage C: why does the sudden transition from the stage B to C occur, and why is the period of the stage-C superhump constant?

PoS(DIM50th2025)010

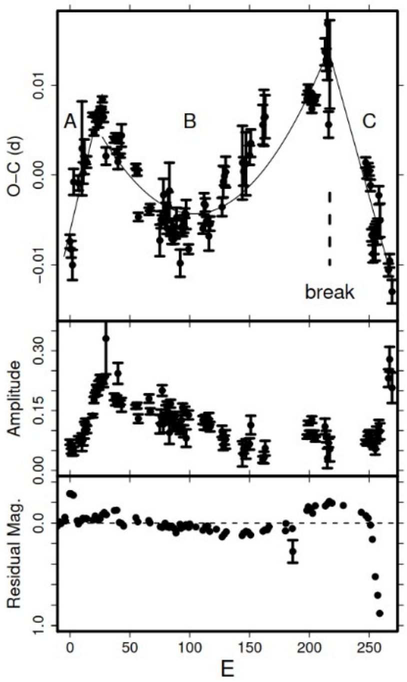

Figure 2: (top) O-C diagram of the superhump maximum timing, (middle) superhump amplitude, and (bottom) superhump amplitude, (bottom) superoutburst light curve after subtraction of a linear decay trend. The horizontal axis represents the superhump cycle (E) starting from the first observed superhump. This figure is Figure 3 in [9].

2.2 A New Method for Mass Ratio Estimation

Kato & Osaki [11] proposed that the mass ratio ($q \equiv M_2/M_1$) can be rather accurately estimated by the excess of the stage-A superhump period and orbital period ($\epsilon^* \equiv (P_{\rm SH} - P_{\rm orb})/P_{\rm orb}$). This idea is based on the formulation of the dynamical precession rate given by Hirose & Osaki [12] and the hypothesis that the stage-A superhump period is determined by the precession rate at the 3:1 resonance radius [10]. Kato & Osaki [11] gave an approximate formula of q in the range of $0.025 \le q \le 0.394$:

$$q = -0.0016 + 2.60\epsilon^* + 3.33(\epsilon^*)^2 + 79.0(\epsilon^*)^3, \tag{1}$$

where the maximum error in q is estimated to be 0.0004. Kato & Osaki[11] checked the validity of this method by comparison of the q value by this method and that by the eclipse analysis (see also [13]).

While the mass ratio is a basic parameter of binaries, accurate estimation of it has been difficult, since it requires observation of the eclipse profile or radial velocity of the secondary star in CVs in quiescence. In contrast, we can estimate the mass ratio by observations of the early superhumps and stage-A superhumps in dwarf novae in superoutburst, since the early superhump period is almost equal to the orbital period [14]. The new and easy method has contributed to increases of the number of DNe with an accurately measured mass ratio.

PoS(DIM50th2025)010

2.3 Standstill and superoutburst in NY Ser

NY Ser is a so-called "in-the-gap" SU UMa star with a superhump period of 2.5 hr and a supercycle of about 100 days [15]. Two standstills were found in the 2018 light curve of this star [16].

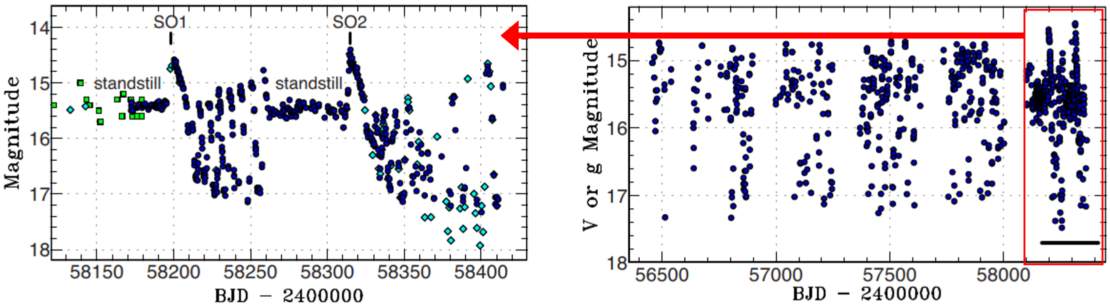

Figure 3: (right) ASAS-SN light curve in V and g bands of NY Ser from 2015 to 2018. (left) Enlarged light curve in 2018. Two superoutbursts occurred directly following standstills. This figure was created based on Figures 1 and 2 in [16].

Both superoutbursts in 2018 rose directly from the immediately prior standstills. The second standstill clearly started during the decay from the prior normal outburst, as often observed in Z Cam stars. While no superhumps were observed during the standstills, superhump evolution apparently began at a very early phase of the second superoutburst rise from the standstill (see E-figure 4 in [16]).

These observed features suggest that 1) the mass transfer rate in NY Ser is close to the limit for the thermally stable disk[1], 2) the 3:1 resonance was excited as the disk expanded to the resonance radius during standstills, and 3) a superoutburst is triggered by the tidal instability.

Related to NY Ser, we also note that RZ LMi, an ER UMa-type dwarf nova near the period minimum was observed to behave like a permanent superhumper intermittently (Kato et al.[17]).

2.4 Long period SU UMa stars

Long P_{orb} SU UMa stars have been discovered so far, e.g. TU Men (P_{orb} = 2.8 hr [18]). Some of them have been proved to have an evolved secondary star, e.g. CRTS J035905.9+175034 [19], and the relationship between orbital period and mass ratio, assuming the secondary star is a main-sequence star, does not apply to these stars.

However, Kato & Vanmunster [20] discovered a long P_{orb} SU UMa star, SDSS J094002.56+274942.0 with a P_{SH} of 4.38 hr. The superhumps had fully evolved by 6 days from the superoutburst maximum. Shallow eclipses were observed during the superoutburst with the orbital period of 3.92 hr. Using P_{orb}, P_{SH} and eclipses, a mass ratio of 0.39(3) and an inclination of 70.5(5)deg were obtained. The Gaia parallax and 2MASS observations support an idea of a main-sequence secondary star in this system, and this idea can explain ellipsoidal modulations observed during quiescence by ZTF and ATLAS (see [21]).

---

[1] A problem remains unsolved that why this star has such a high mass transfer rate even in the period gap.

PoS(DIM50th2025)010

Numerical simulations have indicated the upper limit of the mass ratio for development of the eccentricity by the 3:1 resonance is 0.25 [22] or 0.33 [23]. This discovery of such a high mass-ratio SU UMa star, however, suggests that the eccentricity can grow under a weak tidal effect and would request a reanalysis of the basis of the 3:1 resonance.

2.5 Early Superhumps in WZ Sge stars

Early superhumps are observed exclusively in the very early phase of WZ Sge-type superoutbursts and are regarded as one of the criteria for classification as a WZ Sge-type dwarf nova [24, 25]. They exhibit double-peaked shapes and a period nearly equal to $P_{\rm orb}$. The amplitude of the early superhumps depends on the inclination, suggesting that early superhumps are geometrical phenomena (see e.g. [26]).

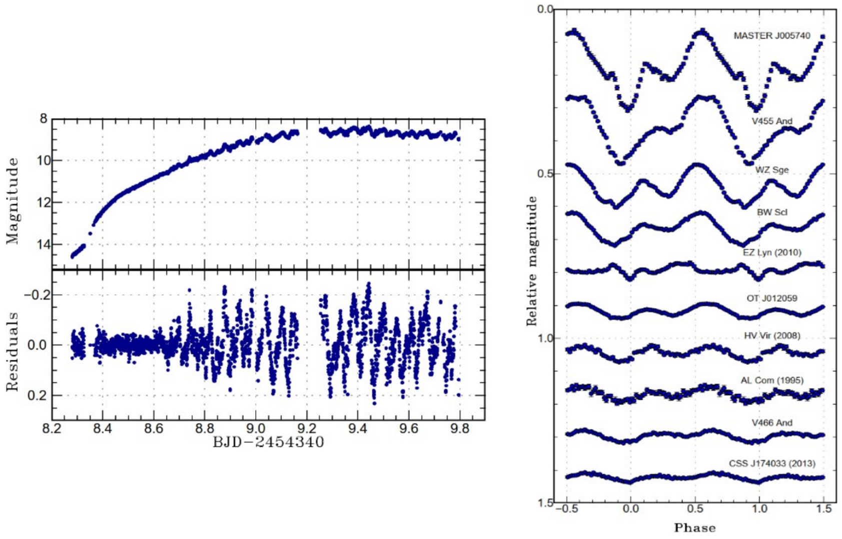

Figure 4: (upperleft) Light curve of two days around the superoutburst maximum in a WZ Sge star V455 And in 2007. (lowerleft) Its detrended one. The evolution of the early superhumps in a very short time (< one day) was clearly observed. (right) Folded superhump profiles in different objects and superoutburst. All have double-peaked shapes, though the details of these profiles are slightly different. This figure was created based on Figures 11 and 12 in [24].

In the TTI model, Osaki & Meyer [27] explained that the early superhump appears due to the 2:1 resonance [28, 29]. The 2:1 resonance radius is smaller than the tidal truncation radius only in systems having a very small mass ratio ($q < 0.08$), and the growth rate of the 2:1 resonance is much larger than the 3:1 resonance. These features naturally explain that early superhumps are observed only in WZ Sge stars before the (ordinary) superhumps appear. Uemura et al. [30] developed a method to reconstruct the vertically extended disk by modelling multi-color light curves of early superhumps under an assumption of self-occultation (for an application of this method, e.g. [26]).

2.6 Long period WZ Sge stars

An outburst of ASASSN-16eg was first observed in 1996 [31]. The overall light curve shown in Fig. 5(a) seems truly a type-C superoutburst (a superoutburst followed by only one short

PoS(DIM50th2025)010

rebrightening) of WZ Sge-type DNe. Both of early superhumps and ordinary superhumps were observed (Fig. 5), and the periods of the early superhump and ordinary superhump were 109 and 115 min. The mass ratio was estimated to be $q = 0.166(2)$ by using the period excess method of the early superhump introduced above. This mass ratio is normal for its orbital period. Wakamatsu et al.[31] listed other SU UMa-type dwarf novae which showed WZ Sge-like superoutbursts so far.

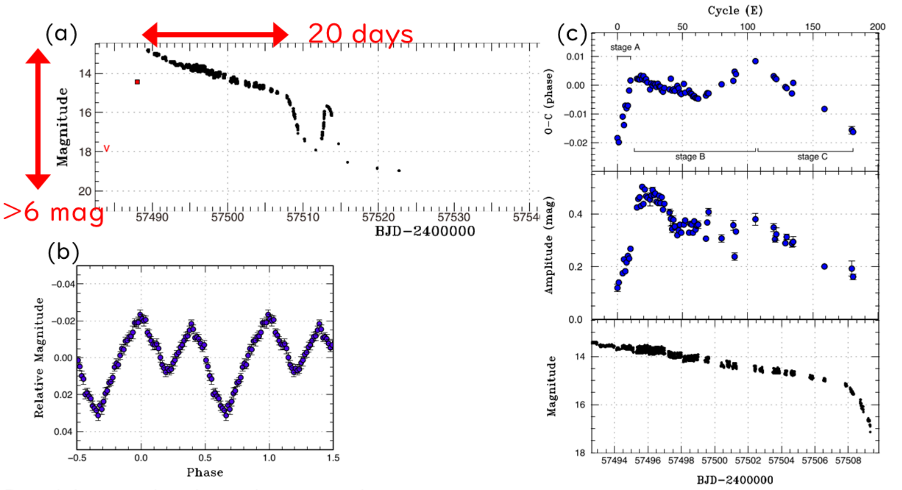

Doubly peaked early superhumps Typical evolution of superhumps

Figure 5: (a) Long-term light curve of ASASSN-16eg during the superoutburst in 2016, which is a typical one of WZ Sge stars. (b) Folded light curve of early superhumps having a double-peaked shape. (c) O-C diagram of the superhump maximum timing (upper), amplitude of the superhump, and (c) light curve of the superoutburst having a common horizontal axis. This figure was created based on Figures 1, 2 and 3 in [31].

While the 2:1 resonance radius exceeds the tidal truncation radius, can the TTI model explain WZ Sge-type superoutbursts in such "high-q" systems? This is still an open question. However, such long period "WZ Sge stars" commonly have long superoutburst cycle lengths over 2 years and large outburst amplitude over 6 mag. This suggests that these stars have very low mass transfer rate for their orbital periods. In this case, the mass and angular momentum stored in the disk by the onset of an outburst may be enough for the disk radius to exceed the tidal truncation radius, to reach the 2:1 resonance radius around the superoutburst maximum. Confirmation by theoretical works and numerical simulations are awaited. This topic may be related to that cool gases beyond the Roche-lobe of the white dwarf were detected during a superoutburst in HT Cas [32].

2.7 Negative Superhumps

Negative superhumps have a period slightly shorter than $P_{\rm orb}$ in contrast to (ordinary) superhumps (e.g. [33]), and they have been observed in various types of cataclysmic variables, such as old novae (e.g. [34]), nova-likes (e.g. [35]), dwarf novae (e.g. [36]), AM CVn stars (e.g. [37]), and so on. An example is exhibited in figure 6. Negative superhumps have the following features: 1) observed in CVs regardless of $P_{\rm orb}$ and q, 2) observed regardless of the state, namely, quiescence, outburst, and standstill, 3) co-existence with (ordinary) superhumps, and 4) unpredictable timings of appearance and disappearance.

PoS(DIM50th2025)010

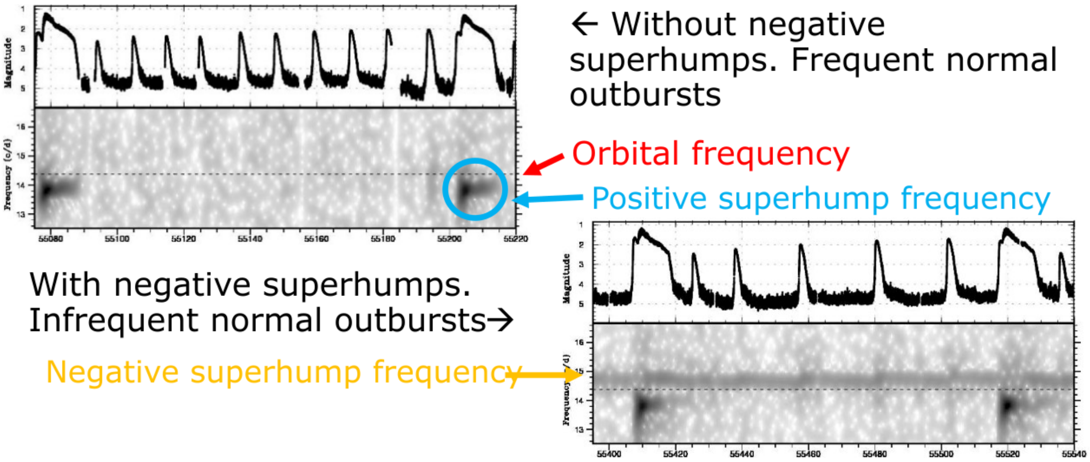

← Without negative superhumps. Frequent normal outbursts

Orbital frequency

Positive superhump frequency

With negative superhumps. Infrequent normal outbursts→

Negative superhump frequency

Figure 6: (upperleft) Kepler light curve of an SU UMa star V1504 Cyg and its dynamic power spectra. Only ordinary superhumps were observed during the superoutbursts. (lowerright) The same, but in the the term when negative superhumps were observed as well as ordinary superhumps. Normal outbursts occurred less frequently in this term. This figure was created based on Figure 3 in [38].

Theoretically, a tilted accretion disk is known to show retrograde precession (e.g. [39]). The period of the negative superhump is explained by the synodic period between the orbital motion and the retrograde precession of the disk (e.g. [40]). The difference of the normal outburst frequency is attributed to the difference of the impact point of the mass stream on the disk [38]. Since disk expansion leads to an increase in the negative superhump frequency [41], variations of the negative superhump period provides insight into disk expansion/shrinkage. Recently, a new subgroup of dwarf novae has been established, called "IW And"-type ([42–44]), which are characterized by the light curves of standstills with oscillations and outbursts directly rising from the standstill. Numerical simulations trying to reproduce the IW And-type behavior by a combination of the thermal instability and tilted disk has been performed [45, 46].

3. Superhumps in related objects

3.1 Superhumps in an intermediate polar CC Scl

Intermediate polars (IPs) have an accretion disk, the inner part of which is truncated by strong magnetic fields on the white dwarf ([47] for a review of IPs,). Some of DNe below the period gap have been proposed or identified to be intermediate polars. CC Scl is an example, whose $P_{\rm orb}$, $P_{\rm SH}$, and spin period were estimated to be 1.4 hr [48, 49], 1.44 hr [50, 51], and 389.5 s [52].

The whole light curve of the superoutburst in CC Scl mimics that of ordinary SU UMa stars (figure 7), which suggests that the TTI model is applicable to IPs if the mass and angular momentum are stored, enough for the disk radius to reach the 3:1 resonance radius, before the onset of a precursor [51]. The duration of the superoutburst is, however, 8 days at most, slightly shorter than a typical value of SU UMa stars, which may be due to truncation of the inner part of the accretion disk [50]. Although the stage-A superhumps were missed, the stage-B and -C superhumps were continuously observed. The transition from the stage B to C occurred about three days after the rapid decay from

PoS(DIM50th2025)010

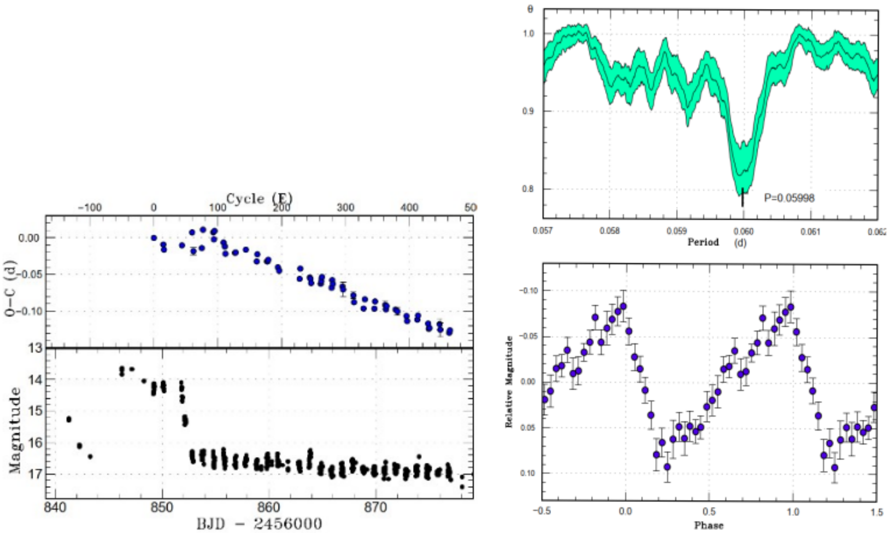

Figure 7: (left) Light curve of the precursor and superoutburst in CC Scl in 2014 (lower) and $O - C$ diagram of the superhump maximum timing in the same horizontal axis (upper). (right) Θ diagram of a PDM analysis for superhumps (upper) and superhump light curve folded by the resultant period. This figure was created based on Figures 1 and 2 in [51].

the superoutburst, while this transition usually occurs before the rapid decay in ordinary SU UMa stars. This implies that the stage C superhumps originate from the outermost part of the accretion disk [51].

3.2 Superhumps in AM CVn Stars

AM CVn stars are a kind of CVs but have a He star or a white dwarf as the secondary ([53, 54] for reviews of AM CVn stars). Superhumps and negative superhumps have been observed also in AM CVn stars, and the behavior of them is basically the same as that of H-rich CVs in a variety of types: nova-likes including permanent superhumpers, Z Cam stars, ER UMa stars and SU UMa stars. Transitions between the states in some of AM CVn stars have been observed (e.g. [55, 56]).

We here introduce an AM CVn star NSV1440. Two superoutbursts were observed in 2015 and 2017 [57], and this star is the first AM CVn star showing light curves analogous to those of type-E superoutbursts and rebrightenings observed in H-rich WZ Sge stars (see [24]). The early and stage-A superhump periods in the 2015 superoutburst were 36.33(1) min and 36.98(3) min, respectively. The mass ratio calculated by using the period-excess method was $q = 0.045(2)$. The orbital period of this star was photometrically measured to be $P_{\rm orb} = 36.56(3)$ min [58]. By substituting this orbital period, the period-excess method gives $q = 0.029(3)$. In either case, NSV 1440 is certainly in the very late stage of the CV evolution, like WZ Sge stars showing type-E superoutbursts. This confirms that the DIM, originally developed for H-rich disks, is also applicable to He-rich disks. Recently, analyses of such outbursts in six long-$P_{\rm orb}$ AM CVn stars clarified that all outbursts have very similar features, especially in the long fading tail following the rebrightening phase [59].

PoS(DIM50th2025)010

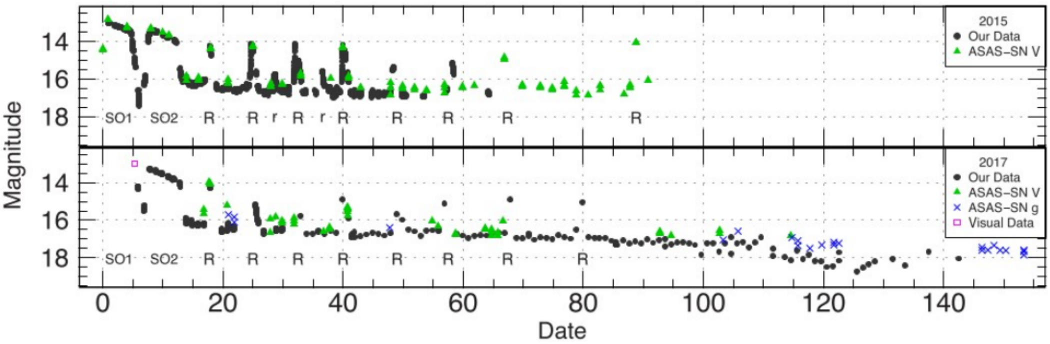

Figure 8: Light curves of the 2015 and 2017 superoutbursts in NSV 1440 in the upper and lower panels. These mimic the type-E superoutburst (double superoutburst divided by a dip) and rebrightenings in WZ Sge stars. This figure is Figures 1 in [57].

3.3 Superhumps in black hole X-ray binaries

As the similarity between the outburst light curves of soft X-ray transients and those of WZ Sge-type dwarf novae has been pointed out (e.g. [60]), superhump-like optical variations have been reported in several black hole X-ray binaries, e.g. KV UMa [61–63]. During the 2018 outburst of the black hole X-ray binary MAXI J1820+070, a clear transition from stage A to stage B superhumps was observed for the first time [64]. The characteristics of the $O-C$ diagram of superhump maxima and the amplitude evolution closely resemble those seen in SU UMa-type dwarf novae.

The mass ratio was estimated to be 0.066(1) using the period-excess method, based on the stage-A superhump period and the orbital period [65]. The black hole mass was estimated to be 7.3-10.8 $M_\odot$, consistent with the value of $8.48^{+0.79}_{-0.72}$ $M_\odot$ derived from the rotational velocity. Furthermore, the superhump stage transition occurred about 5 days earlier than the transition from the hard to soft X-ray state. This behavior can be naturally interpreted in terms of inward propagation of enhanced viscosity and the associated viscous timescale [64].

These results indicate that the TTI model is applicable to outbursts in black hole X-ray binaries, despite the presence of strong gravity and intense X-ray irradiation. However, the large superhump amplitude of approximately 0.8 mag and the absence of detectable color variation during the superhump phase observed in this system remain unresolved issues.

4. Conclusion

The disk instability model, supplemented by geometric effects, has evolved into a remarkably successful framework for interpreting the diverse phenomenology of superhumps in cataclysmic variables. Systematic observations have established the stage A-B-C evolution of superhumps, enabled a new and practical method for estimating binary mass ratios, and revealed unexpected behaviors such as standstill-triggered superoutbursts, high-mass-ratio SU UMa stars, long-period WZ Sge-like systems, and the widespread occurrence of negative superhumps.

At the same time, these observations expose important theoretical challenges. The origin of period changes during stage B, the abrupt transition to stage C, the growth of eccentricity at

PoS(DIM50th2025)010

unexpectedly high mass ratios, and the excitation of the 2:1 resonance in long-period systems all require further investigation through analytical work and numerical simulations. The detection of superhumps in intermediate polars and AM CVn stars further demonstrates that the essential physics of the disk instability model is applicable across a wide range of disk compositions, magnetic environments, and evolutionary stages.

The progress reviewed here underscores the unique role of superhumps as a diagnostic of accretion-disk structure and dynamics. Insights gained from cataclysmic variables provide a valuable foundation for understanding accretion phenomena on longer timescales and larger spatial scales, including those in X-ray binaries and active galactic nuclei.

Acknowledgments

This work is partly supported by JSPS KAKENHI Grant Number 24H00248. We thank the amateur observers who have provided valuable data to VSNET, AAVSO, and other organizations. Furthermore, the availability of ground-based survey data and data from space telescopes Kepler and TESS has greatly contributed as the foundation for the research introduced here.

References

[1] B. Warner, *Cataclysmic Variable Stars*, Cambridge University Press (1995).

[2] Y. Osaki, *An accretion model for the outbursts of U Geminorum stars*, PASJ, 26, 429 (1974).

[3] N. Vogt, *Photometric study of the dwarf nova VW Hydri*, A&A, 36, 369 (1974).

[4] B. Warner, *Stars that GO hump in the night – the SU UMa stars*, in *Interacting Binaries*, P.P. Eggleton and J.E. Pringle, eds., p. 367, 1985.

[5] Y. Osaki, *A model for the superoutburst phenomenon of SU Ursae Majoris stars*, PASJ, 41, 1005 (1989).

[6] Y. Osaki, *Dwarf-nova outbursts*, PASP, 108, 39 (1996).

[7] Y. Osaki, *A brief history of the disk instability model in cataclysmic variable stars*, in proceedings of "The 50th Anniversary Workshop of the Disk Instability Model in Compact Binary Stars" PoS(DIM50th2025)002 (2026).

[8] J. Patterson, G. Thomas, D.R. Skillman and M. Diaz, *The 1991 V603 Aquilae campaign – superhumps and P-dots*, ApJS, 86, 235 (1993).

[9] T. Kato, A. Imada, M. Uemura, D. Nogami, H. Maehara, R. Ishioka et al., *Survey of period variations of superhumps in SU UMa-type dwarf novae*, PASJ, 61, S395 (2009).

[10] Y. Osaki and T. Kato, *Study of superoutbursts and superhumps in SU UMa stars by the Kepler light curves of V344 Lyrae and V1504 Cygni*, PASJ, 65, 95 (2013).

[11] T. Kato and Y. Osaki, *New method to estimate binary mass ratios by using superhumps*, PASJ, 65, 115 (2013).

PoS(DIM50th2025)010

[12] M. Hirose and Y. Osaki, *Hydrodynamic simulations of accretion disks in cataclysmic variables – superhump phenomenon in SU UMa stars*, PASJ, 42, 135 (1990).

[13] T. Kato, *Evolution of short-period cataclysmic variables: implications from eclipse modeling and stage a superhump method (with new yearś gift)*, VSOLJ Variable Star Bulletin, 89 (2022).

[14] R. Ishioka, M. Uemura, K. Matsumoto, H. Ohashi, T. Kato, G. Masi et al., *First detection of the growing humps at the rapidly rising stage of dwarf novae AL Com and WZ Sge*, A&A, 381, L41 (2002).

[15] D. Nogami, T. Kato, H. Baba and S. Masuda, *Discovery of the first in-the-gap SU UMa-type dwarf nova, NY Serpentis (=PG 1510+234)*, PASJ, 50, L1 (1998).

[16] T. Kato, E.P. Pavlenko, N.V. Pit, K.A. Antonyuk, J.V. Babina, A.V. Baklanov et al., *Discovery of standstills in the SU UMa-type dwarf nova NY Serpentis*, PASJ, 71, L1 (2019).

[17] T. Kato, R. Ishioka, K. Isogai, M. Kimura, A. Imada, I. Miller et al., *RZ Leonis Minoris bridging between ER Ursae Majoris-type dwarf nova and nova-like system*, PASJ, 68, 107 (2016).

[18] B. Stolz and R. Schoembs, *The SU UMa star TU Mensae*, A&A, 132, 187 (1984).

[19] C. Littlefield, P. Gamavich, M. Kennedy, P. Szkody and Z. Dai, *A comprehensive K2 and ground-based study of CRTS J035905.9+175034, an eclipsing su uma system with a large mass ratio*, AJ, 155, 232 (2018).

[20] T. Kato and T. Vanmunster, *SDSS J094002.56+274942.0: an SU UMa star with an orbital period of 3.92 hours and an apparently unevolved secondary*, VSOLJ Variable Star Bulletin, 114 (2023).

[21] T. Kraijci and P. Wils, *SDSS J094002.56+274942.0: an SU UMa star with an orbital period of 3.92 hours and an apparently unevolved secondary*, Journal of AAVSO, 38, 33 (2010).

[22] R. Whitehurst, *Numerical simulations of accretion disks. I - superhumps - a tidal phenomenon of accretion disks*, MNRAS, 232, 35 (1988).

[23] J.R. Murray, *The precession of eccentric discs in close binaries*, MNRAS, 314, L1 (2000).

[24] T. Kato, *WZ Sge-type dwarf novae*, PASJ, 67, 108 (2015).

[25] Y. Tampo, *WZ Sge-type dwarf novae: an extreme laboratory in cataclysmic variables*, in proceedings of "The 50th Anniversary Workshop of the Disk Instability Model in Compact Binary Stars" PoS(DIM50th2025)014 (2026).

[26] Y. Tampo, K. Isogai, N. Kojiguchi, M. Uemura, T. Kato, T. Tordai et al., *PNV J00444033+4113068: Early superhumps with 0.7 mag amplitude and non-red color*, PASJ, 74, 1287 (2022).

PoS(DIM50th2025)010

[27] Y. Osaki and F. Meyer, *Early humps in WZ Sge stars*, A&A, 383, 574 (2002).

[28] D.N.C. Lin and J. Papaloizou, *Tidal torques on accretion discs in binary systems with extreme mass ratios*, MNRAS, 186, 799 (1979).

[29] S.H. Lubow, *A model for tidally driven eccentric instabilities in fluid disks*, ApJ, 381, 259 (1991).

[30] M. Uemura, T. Kato, T. Ohshima and H. Maehara, *Reconstruction of the structure of accretion disks in dwarf novae from the multi-band light curves of early superhumps*, PASJ, 64, 92 (2012).

[31] Y. Wakamatsu, K. Isogai, M. Kimura, T. Kato, T. Vanmunster, G. Stone et al., *ASASSN-16eg: New candidate for a long-period WZ Sge-type dwarf nova*, PASJ, 69, 89 (2017).

[32] V.V. Neustroef and S.V. Zharikov, *Voracious vortices in cataclysmic variables. II. evidence for the expansion of accretion disc material beyond the roche lobe of the accretor in HT Cassiopeia during its 2017 superoutburst*, A&A, 642, A100 (2020).

[33] D. Harvey, D.R. Skillman, J. Patterson and F.A. Ringwald, *Superhumps in cataclysmic binaries. V. V503 Cygni*, PASP, 107, 551 (1995).

[34] A. Bruch, *TESS light curves of cataclysmic variables -II- superhumps in old novae and novalike variables*, MNRAS, 519, 352 (2023).

[35] M. Veresvarska, S. Scaringi, C. Littlefield, D. de Martino, C. Knigge, J. Paice et al., *DW Cnc: a micronova with a negative superhump and a flickering spin*, MNRAS, 539, 2424 (2025).

[36] A. Joshi, C. Tappert, M. Catelan, L. Schmidtobreick and M. Singh, *A tale of three cataclysmic variables with distinct superhumps*, A&A, 702, A70 (2025).

[37] S. Solanki, T. Kupfer, O. Blaes, E. Breedt and S. Scarringi, *Periodicities in the K2 lightcurve of HP Librae*, MNRAS, 500, 1222 (2021).

[38] Y. Osaki and T. Kato, *The cause of the superoutburst in SU UMa stars is finally revealed by Kepler light curve of V1504 Cygni*, PASJ, 65, 50 (2013).

[39] J.C.B. Papaloizou and J.E. Pringle, *The time-dependence of non-planar accretion discs*, MNRAS, 202, 1181 (1983).

[40] M.M. Montgomery and E.L. Martin, *A common source of accretion disk tilt*, ApJ, 722, 989 (2010).

[41] J. Larwood, *On the precession of accretion discs in X-ray binaries*, MNRAS, 299, L32 (1998).

[42] M. Simonsen, *The Z CamPaign: Year 1*, Journal of AAVSO, 39, 66 (2011).

[43] P. Szkody, M. Albright, A.P. Linnell, M.E. Everett, R. McMillan, G. Saurage et al., *A study of the unusual Z Cam systems IW Andromedae and V513 Cassiopeia*, PASP, 125, 1421 (2013).

PoS(DIM50th2025)010

[44] T. Kato, *Three Z Camelopardalis-type dwarf novae exhibiting iw andromedae-type phenomenon*, PASJ, 71, 20 (2019).

[45] M. Kimura, Y. Osaki, T. Kato and S. Mineshige, *Thermal-viscous instability in tilted accretion disks: A possible application to IW Andromeda-type dwarf novae*, PASJ, 72, 22 (2020).

[46] M. Kimura, *Could the thermal instability in the tilted disk be responsible for iw and phenomenon?*, in proceedings of "The 50th Anniversary Workshop of the Disk Instability Model in Compact Binary Stars" PoS(DIM50th2025)012 (2026).

[47] J. Patterson, *The DQ Herculis stars*, PASP, 106, 209 (1994).

[48] A. Chen, D. O'Donoghue, R.S. Stobie, D. Kilkenny and B. Warner, *Cataclysmic variables in the Edinburgh-Cape Blue Object Survey*, MNRAS, 325, 89 (2001).

[49] C. Tappert, T. Augusteijn and J. Maza, *Cataclysmic variables from the Calán-Tololo Survey - I. Photometric periods*, MNRAS, 354, 321 (2004).

[50] P.A. Woudt, B. Warner, A. Gulbis, R. Coppejans, F.-J. Hambsch, A.P. Beardmore et al., *CC Sculptoris: A superhumping intermediate polar*, MNRAS, 427, 1004 (2012).

[51] T. Kato, F.-J. Hambsch, A. Oksanen, P. Starr and A. Henden, *CC Sculptoris: Eclipsing SU UMa-type intermediate polar*, PASJ, 67, 3 (2015).

[52] J.A. Paice, S. Scaringi, N. Castro Segura, A. Sahu, K. Iłkiewicz, D.L. Coppejans et al., *Evolution of spin in the intermediate polar CC Sculptoris*, MNRAS, 531, L82 (2024).

[53] J. Solheim, *AM CVn stars: Status and challenges*, PASP, 122, 1133 (2010).

[54] G. Ramsay, *Outbursts in ultra-compact AM CVn binaries*, in proceedings of "The 50th Anniversary Workshop of the Disk Instability Model in Compact Binary Stars" PoS(DIM50th2025)017 (2026).

[55] J. Patterson, S. Walker, J. Kemp, D. O'Donoghue, M. Bos and R. Stubbings, *V803 Centauri: A helium-rich dwarf nova*, PASP, 112, 625 (2000).

[56] R.K. Honeycutt, B.R. Adams, G.W. Turner, J.W. Robertson, E.M. Ost and J.E. Maxwell, *Light curve of CR Bootis 1990–2012 from the Indiana long-term monitoring program*, PASP, 125, 126 (2013).

[57] K. Isogai, T. Kato, B. Monard, K. Kasai, F.-J. Hambsch, G. Myers et al., *NSV 1440: first WZ Sge-type object in AM CVn stars and candidates*, PASJ 71, 48 (2019).

[58] A. Aungwerojwit, B.T. Gänsicke, E. Breet, S. Arjyotha, J.J. Hermes, F.J. Hambsch et al., *Follow-up on three poorly studied AM CVn stars*, MNRAS, 537, 3078 (2025).

[59] N. Kojiguchi, K. Isogai, Y. Tampo, T. Kato, H. Itoh, B. Manard et al., *Observational study of double superoutbursts in long-orbital-period AM CVn stars*, PASJ, 78, in press (2026).

PoS(DIM50th2025)010

[60] E. Kuulkers, *WZ Sge stars/TOADs and (soft) X-ray transients: close encounters of the same kind*, New Astrnomy, 44, 27 (2000).

[61] R.M. Wagner, C.B. Foltz, T. Shahbaz, J. Casares, P.A. Charles, S.G. Starrfield et al., *The halo black hole x-ray transient XTE J1118+480*, ApJ, 556, 42 (2001).

[62] J.E. McClintock, C.A. Haswell, M.R. Garcia, J.J. Drake, R.I. Hynes, H.L. Marshall et al., *Complete and simultaneous spectral observations of the black hole x-ray nova XTE J1118+480*, ApJ, 555, 477 (2001).

[63] M. Uemura, T. Kato, K. Matsumoto, H. Iwamatsu, R. Ishioka, L.M. Cook et al., *Optical observations of XTE J1118+480 during the 2000 outburst*, PASJ, 54, 285 (2002).

[64] K. Niijima, M. Kimura, T. Wakamatsu, Y. Kato, D. Nogami, K. Isogai, N. Kojiguchi et al., *Optical variability correlated with X-ray spectral transition in the black-hole transient ASASSN-18ey = MAXI J1820+070*, VSOLJ Variable Star Bulletin, 74 (2021).

[65] M.A.P. Torres, J. Vasares, F. Jiménez-Ibarra, T. Muñoz-Darias, M. Armas Padilla, P.G. Jonker et al., *Dynamical confirmation of a black hole in MAXI J1820+070*, ApJ, 882, 21 (2019).

PoS(DIM50th2025)010